
Bayesian Active Learning for Discrete Latent Variable Models

Aditi Jha^{*1,3}, Zoe C. Ashwood^{2,3}, Jonathan W. Pillow^{3,4}

¹Dept. of Electrical and Computer Engineering, Princeton University

²Dept. of Computer Science, Princeton University

³Princeton Neuroscience Institute, Princeton University

⁴Dept. of Psychology, Princeton University

Abstract

Active learning seeks to reduce the number of samples required to estimate the parameters of a model, thus forming an important class of techniques in modern machine learning. However, past work on active learning has largely overlooked latent variable models, which play a vital role in neuroscience, psychology, and a variety of other engineering and scientific disciplines. Here we address this gap in the literature, and propose a novel framework for maximum-mutual-information input selection for learning discrete latent variable regression models. We first examine a class of models known as “mixtures of linear regressions” (MLR). This example is striking because it is well known that active learning confers no advantage for standard least-squares regression. However, we show—both in simulations and analytically using Fisher information—that optimal input selection can nevertheless provide dramatic gains for *mixtures* of regression models; we also validate this on a real-world application of MLRs. We then consider a powerful class of temporally structured latent variable models known as Input-Output Hidden Markov Models (IO-HMMs), which have recently gained prominence in neuroscience. We show that our method substantially speeds up learning, and outperforms a variety of approximate methods based on variational and amortized inference.

1 Introduction

Obtaining labeled data is a key challenge in many scientific and machine learning applications. Active learning provides a solution to this problem, allowing us to identify the most informative data points and thereby minimize the number of examples needed to fit a model. Bayesian active learning, also known as optimal or adaptive experimental design [12, 14, 59], has had a major impact on a variety of disciplines, including neuroscience [17, 18, 28, 35, 39–41, 49, 52, 57], psychology [4, 16, 47, 60, 61], genomics [58] and astronomy [45].

Our problem setting involves a probabilistic model $p(y|\mathbf{x}, \theta)$, in which a parameter vector θ governs the probabilistic relationship between inputs \mathbf{x} and labels or outputs y . We wish to select inputs

*Corresponding author: aditijha@princeton.edu

$\{\mathbf{x}_i\}$ that will allow us to accurately infer θ from the resulting dataset $\{\mathbf{x}_i, y_i\}$. In standard “fixed-design” experiments, the inputs are selected in advance, or drawn randomly from a predetermined distribution. In adaptive or “closed-loop” experiments, by contrast, the inputs are selected adaptively during the experiment based on the measurements obtained so far. Bayesian active learning methods provide a framework for optimally selecting these inputs, where optimality is defined by a utility function that characterizes the specific learning objective [14, 46, 52, 55].

Despite a burgeoning literature, the active learning field has devoted little attention to latent variable models (e.g., [1, 14, 30]). Latent variable models (LVMs) represent a class of highly expressive models with a vast range of applications. In neuroscience in particular, they have provided powerful descriptions of both neural population activity [13, 19, 27, 44, 64, 65] and animal behavior [2, 9, 10, 63].

The key feature of latent variable regression models is that the relationship between inputs \mathbf{x} and output y is mediated by an unobserved or hidden state variable \mathbf{z} , so that we have:

$$\begin{aligned} z &\sim p(z) \\ y \mid \mathbf{x}, z &\sim p(y \mid \mathbf{x}, z), \end{aligned} \tag{1}$$

where $p(z)$ is the prior over the latent variable, and $p(y \mid \mathbf{x}, z)$ characterizes the joint dependence of the system output on the input and latent variable. This structure provides LVMs with the flexibility to describe internal states of the system that cannot be observed directly. However, this flexibility comes with a cost: computing the likelihood (and by extension, the posterior) in LVMs requires marginalizing over the latent variable, $P(y \mid \mathbf{x}) = \sum_z P(y \mid \mathbf{x}, z)P(z)$. This complicates posterior inference and the calculation of expected utility, both of which are required for Bayesian active learning algorithms.

To address this gap in the literature, we introduce a Bayesian active learning framework for discrete latent variable models. We develop methods based on both MCMC sampling and variational inference to efficiently compute information gain and select informative inputs in adaptive experiments. We illustrate our framework with applications to two specific families of latent variable models: (1) a mixture of linear regressions (MLR) model; and (2) input-output Hidden Markov Models (IO-HMM). We compare the efficiency of different methods, including a recent method based on amortized inference using deep networks [23], and show that in both model families our approach provides dramatic speedups in learning over previous methods.

2 Related work

Bayesian active learning methods have been developed for a wide range of different models, from generalized linear models [3, 4, 11, 34, 39–41, 48] to neural networks [14, 15, 17, 18, 25, 36]. One body of work has focused on Bayesian active learning for models with implicit likelihoods [32, 37]. Another recent line of work has focused on general-purpose real-time active learning using amortized inference in deep neural networks, an approach known as Deep Adaptive Design (DAD) Foster et al. [23]. However, the literature on active learning for latent variable models is sparse, limited to a few specific model classes and tasks such as density modeling [14, 30] and state estimation for standard HMMs [1].

The approach we develop here grows out of previous work on Bayesian active learning methods for generalized linear models [4, 31, 39, 40]. However, our contribution is novel because the posterior approximations used in prior work are inapplicable to the latent variable model setting.

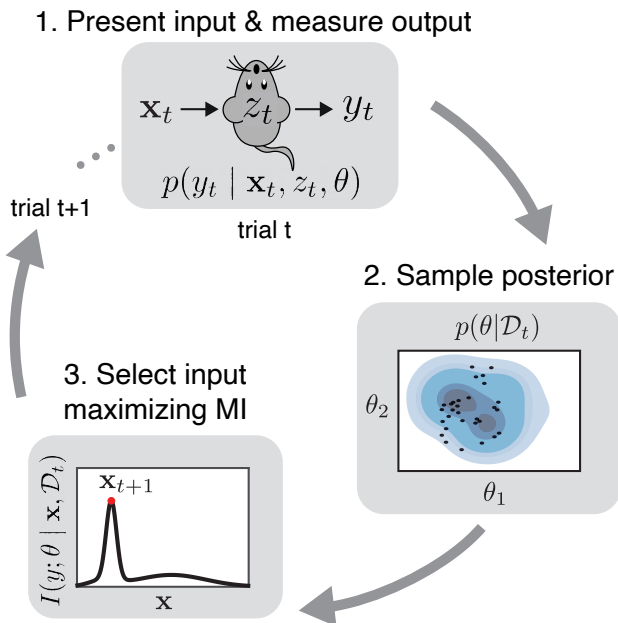


Figure 1: Infomax learning for discrete latent variable models. First, on trial t , present an input \mathbf{x}_t to the system of interest (e.g., a mouse performing a decision-making task) and record its response y_t . We assume this response depends on the stimulus (input) as well as an internal or latent state z_t , as specified by the model $p(y_t | \mathbf{x}_t, z_t, \theta)$. Second, draw samples from the posterior distribution over model parameters θ given the data collected so far in the experiment, $\mathcal{D}_t = \{\mathbf{x}_{1:t}, y_{1:t}\}$. Third, select the input for the next trial that maximizes information gain, or the mutual information between the next response y_{t+1} and the model parameters θ .

3 Bayesian active learning for discrete latent variable models

Figure 1 shows an illustration of Bayesian active learning in the context of a neuroscience experiment. The system or animal receives an input $\mathbf{x} \in \mathbb{R}^D$ on each trial, and generates a response $y \in \Omega$ which may be continuous or discrete. We assume that these responses are described by $p(y | \mathbf{x}, z, \theta)$, where $z \in \{1, \dots, K\}$ denotes a discrete latent variable governing the internal state of the system, characterized by a (possibly structured) prior distribution $p(z)$, and θ denotes the model parameters.

The goal of active-learning is to select inputs that will allow us to infer θ in as few trials as possible. Bayesian active learning formalizes this in terms of a utility function that specifies the learning goal (e.g., maximizing information, minimizing prediction error). Here we select mutual information between y_t and the parameters θ conditioned on the input, giving the selection rule:

$$\mathbf{x}_{t+1} = \arg \max_{\mathbf{x}} I(\theta; y_t | \mathbf{x}, \mathcal{D}_t). \quad (2)$$

This popular choice of utility function gives rise to a large family of Bayesian active learning methods commonly known as “infomax learning” [4, 31, 39, 40, 46, 49, 52]. The challenge in applying infomax learning to latent variable models is that the posterior distribution, which is necessary for computing information, is generally not available in closed form. To overcome this challenge, we consider two different approaches, one based on sampling and another based on variational inference (VI) [8]. For the sampling-based approach, we use Gibbs sampling to obtain an alternating chain of samples from the conditional distributions over latent variables and the model parameters. We can use these parameter samples, $\{\theta^j\}_{j=1}^M \sim p(\theta | \mathcal{D}_t)$, to evaluate the mutual information between y_t and θ

conditioned on input \mathbf{x}_t as follows (see S1 for derivation):

$$I(\theta; y | \mathbf{x}, \mathcal{D}_t) \approx \frac{1}{M} \sum_{j=1}^M D_{KL} (p(y | \theta^j, \mathbf{x}) || p(y | \mathbf{x}, \mathcal{D}_t)), \quad (3)$$

where D_{KL} is the Kullback-Leibler divergence, and $p(y | x, \mathcal{D}_t) \approx \frac{1}{M} \sum_{j=1}^M p(y | \theta^j, \mathbf{x})$ is the average predictive probability across samples, where these predictive probabilities are in turn computed by marginalizing over the latent: $p(y | \theta^j, \mathbf{x}) = \sum_{k=1}^K p(z = k | \theta^j, \mathbf{x}) p(y | z = k, \theta^j, \mathbf{x})$

Equation 3 makes clear that information-based active learning can be equivalently seen as comparing the prediction of the models given by each of the M samples, $p(y | \theta^j, \mathbf{x})$, with the average model prediction $p(y | x, \mathcal{D}_t)$, and choosing the input which maximizes the average difference between predictions of individual models and the consensus model. This shows that infomax learning can also be seen as a form of “query-by-committee”, a well-known method in the active learning literature [56].

For the VI-based method, we compute a variational approximation to the posterior, which is faster than Gibbs sampling but may be less accurate. We then draw samples from the (approximate) variational posterior, and use those samples to evaluate mutual information as described above (eq. 3).

4 Mixture of linear regressions (MLR)

The mixture of linear regressions (MLR) model has a rich history in machine learning [6, 24, 43]. It consists of an independent mixture of K distinct linear-Gaussian regression models (Fig. 2A). Given an input, $\mathbf{x} \in \mathbb{R}^D$, the corresponding output observation $y \in \mathbb{R}$ arises from one of the K components as determined by the latent state $z \in \{1, \dots, K\}$. Formally, it can be written:

$$\begin{aligned} z_t &\sim \text{Cat}(\pi) \\ y_t | (\mathbf{x}_t, z_t = k) &\sim \mathcal{N}(\mathbf{x}_t^\top \mathbf{w}_k, \sigma^2) \end{aligned} \quad (4)$$

where $\pi \in \Delta^{K-1}$ denotes a discrete or categorical distribution over the set of K mixing components, and $\mathbf{w}_k \in \mathbb{R}^D$ denotes the weights of the linear regression model in state k . The model parameters to be learned are thus given by $\theta = \{\mathbf{w}_{1:K}, \pi\}$.

Fisher information analysis

Before describing our algorithm, we pause to ask whether there is any hope that infomax learning will be helpful for the MLR model. In the standard linear-Gaussian regression model, it is straightforward to see that posterior covariance of model parameters, given by $(C_0^{-1} + \frac{1}{\sigma^2} \sum_{t=1}^T \mathbf{x}_t \mathbf{x}_t^\top)^{-1}$ where C_0 is the prior covariance, is independent of the outputs $\{y_t\}$. This means that an optimal design can be planned out prior to the experiment, and there is no benefit to taking into account the output y_t when selecting the next input \mathbf{x}_{t+1} [11, 46]. Intriguingly, this property does not hold for the MLR model.

To quantify the asymptotic performance of infomax learning for the MLR model, and to gain insight into which inputs are most informative, we can compute the Fisher information, which sets asymptotic limits on the error in estimating the parameters via the Cramer-Rao bound [48].

The Fisher information matrix for a model with parameters θ is a matrix with i, j 'th element $J_{jk} = \mathbb{E} \left[\left(\frac{\partial}{\partial \theta_j} \log p(y|\mathbf{x}, \theta) \right) \left(\frac{\partial}{\partial \theta_k} \log p(y|\mathbf{x}, \theta) \right) \right]$, where expectation is taken with respect to $p(y|\mathbf{x}, \theta)$. For an MLR model in D dimensions with K components, the Fisher information matrix for the weights given an input vector \mathbf{x} is a $KD \times KD$ matrix whose i, j 'th block is given by:

$$J_{[i,j]}(\mathbf{x}) = \frac{1}{\sigma^4} \mathbb{E}[(y - \mathbf{x}^\top \mathbf{w}_i)(y - \mathbf{x}^\top \mathbf{w}_j)p(z = i | y, \mathbf{x}, \theta)p(z = j | y, \mathbf{x}, \theta)] \mathbf{x}\mathbf{x}^\top, \quad (5)$$

where expectation is taken with respect to the marginal distribution $p(y | \mathbf{x}, \theta)$ (see S6 for details). Although this expectation cannot generally be computed analytically [5], we can compute it for the two extreme cases of interest: (1) perfect identifiability, when the response y gives perfect information about the latent variable; and (2) non-identifiability, when the response provides no information about the latent variable.

To illustrate these cases, Fig. 2B shows an example MLR model with two 2D weight vectors pointing in opposite directions along the x_1 axis. If observation noise variance σ^2 is small, a unit vector input with 0 degree orientation renders the latent state perfectly identifiable, since the response will be large and positive if $z = 1$ and negative if $z = 2$. On the other hand, an input at 90 or 270 degrees gives rise to non-identifiability; these inputs are orthogonal to both \mathbf{w}_1 and \mathbf{w}_2 , so observing the output y will provide no information about which component produced it.

In the case of perfect identifiability, the Fisher information matrix simplifies to a block diagonal matrix with $\frac{1}{\sigma^2} \pi_i \mathbf{x}\mathbf{x}^\top$ in its i th block (see S6). The trace of the Fisher information matrix, which quantifies the total Fisher information provided by this input, is $\frac{1}{\sigma^2} \|\mathbf{x}\|^2$, which remarkably, is the same Fisher information as in the standard (non-mixture) linear regression model. In the case of non-identifiability, on the other hand, the Fisher information is a rank-1 matrix with block i, j given by $\frac{1}{\sigma^2} \pi_i \pi_j \mathbf{x}\mathbf{x}^\top$. In the case where all class prior probabilities are equal ($\pi_i = 1/K \forall i$), the trace is only $\frac{1}{K\sigma^2} \|\mathbf{x}\|^2$, revealing that non-identifiable inputs can provide as little as $1/K$ as much Fisher information as inputs with perfect identifiability. The dependence on the number of components, K , is worth noting as it suggests that active learning may have a greater impact for models with more components.

Figure 2C shows the (numerically computed) Fisher information as a function of input angle for the MLR model shown in panel B, for different noise levels σ^2 . This confirms the analytic result that Fisher information for this 2-state model is 1/2 its maximal value for inputs in the ‘‘non-identifiability’’ region, and shows that the sub-optimal input region grows wider as noise variance increases. This confirms that active learning can improve MLR model fitting, and clarifies which inputs are most informative.

Infomax learning algorithm for MLR

To perform infomax learning for MLR models, we use Gibbs sampling [7] to obtain samples from the posterior over model parameters. This involves sampling from the joint distribution over the latents z and the model parameters $\theta = \{\mathbf{w}_{1:K}, \pi\}$, conditioned on the data. As an alternate strategy, we also draw samples of the model parameters from a variational approximation to its posterior (see S2 and S3 for details). Next, using M samples of the model parameters, $\{\mathbf{w}_{1:K}^j, \pi^j\}_{j=1}^M$, we compute the mutual information between the system’s output and the parameters (Eq. 3) for a grid of candidate inputs by substituting the likelihood term, $p(y | \theta^j, \mathbf{x}, \mathcal{D}_t) = \sum_{k=1}^K \pi_k^j \mathcal{N}(y | \mathbf{w}_k^j \cdot \mathbf{x}, 1)$, into Eq. 3. Finally, we select the input \mathbf{x} that maximizes Eq. 3 and present it to the system on the next trial.

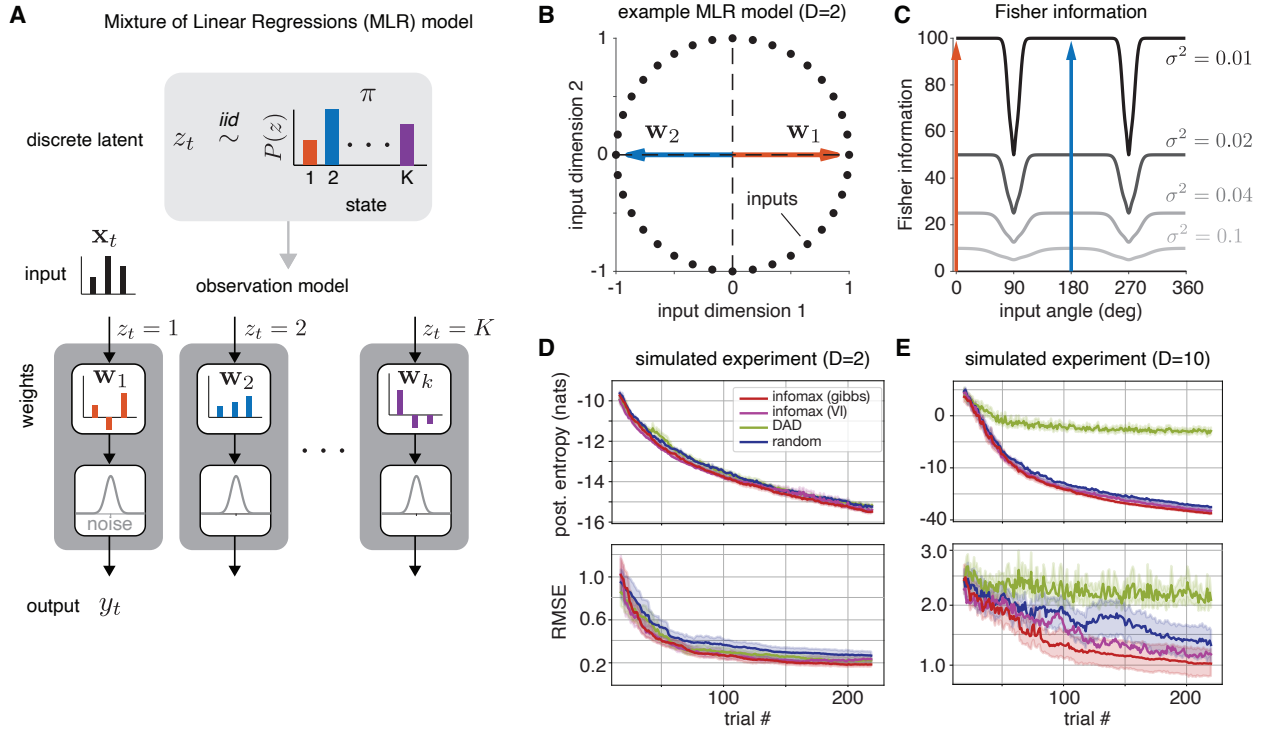


Figure 2: Infomax learning for mixture of linear regressions (MLR) models. **(A)** Model schematic. At time step, t , system is in state $z_t = k$ with probability π_k . The system generates output y_t using state-dependent weights \mathbf{w}_k and independent additive Gaussian noise (Eq. 4). **(B)** Example 2-state model with two-dimensional weights $\mathbf{w}_1 = (1, 0)$ and $\mathbf{w}_2 = (-1, 0)$. We consider possible inputs on the unit circle, which are the information-maximizing inputs for linear Gaussian models under an L_2 norm constraint. **(C)** Fisher information as a function of the angle between \mathbf{w}_1 and the input presented to the system, for different noise variances σ^2 . **(D)** Comparison between infomax active learning (using Gibbs sampling and VI), DAD and random sampling for the 2D MLR model shown above with mixing probabilities $\pi = [0.6, 0.4]$ and noise variance $\sigma^2 = 0.1$. Error bars reflect 95% confidence interval (standard error) of the mean across 20 experiments. **(E)** Performance comparison for the same 2-state model but with 10-dimensional weight vectors and inputs. The possible inputs to the system were uniform samples from the 10-D unit hyper-sphere.

Experiments with MLRs

To evaluate our active learning framework for MLRs, we first perform two simulations. In our first experiment, illustrated in Fig. 2B, the set of possible inputs lie on a unit circle, 10° apart. At any trial, an input from this set is presented and the output arises from one of $K = 2$ regression models. We fix the state probabilities as $\pi = [0.6, 0.4]$. The regression models have the form: $y_t = \mathbf{w}_k^\top x_t + \epsilon$ where we fix the generative parameters as: $\mathbf{w}_1 = [-1, 0]$, $\mathbf{w}_2 = [1, 0]$ and $\epsilon \sim \mathcal{N}(0, 0.1)$. Our second experiment follows the same setup, but selects input from a set of 1000 candidate points sampled uniformly on the 10-D hyper-sphere. The output again arises from one of the two regression models, now with weights oriented along the first two major axes, $\mathbf{w}_1 = [1, 0, \dots, 0]$ and $\mathbf{w}_2 = [0, 1, 0, \dots, 0]$, and mixing weights $\pi = [0.6, 0.4]$.

The task at hand is to learn the generative parameters of the model: *i.e.* $\{\mathbf{w}_1, \mathbf{w}_2, \pi\}$. We compare several input-selection strategies including our infomax learning methods (using gibbs sampling and

variational inference), a random sampling approach which selects inputs uniformly from the set of all possible inputs, and Deep Adaptive Design (DAD) by Foster et al. [23]. We adapted the code for DAD to use it for input selection in MLRs (details in S4). In all cases, after input selection, at each trial we infer the model parameters using Gibbs sampling.

A natural quantity to track during infomax learning is the entropy of the posterior distribution over the model parameters θ [4], which we approximate as $\log |\text{cov}(\theta)|$. We compute the sample-estimate of this posterior entropy using the M samples obtained from Gibbs sampling at every trial. We find that the posterior entropy of the model parameters decreases fastest for infomax Gibbs sampling as compared to the other methods (top panel of Fig. 2D). In 10-d, this difference is even more prominent (top panel of Fig. 2E). We also track the root mean squared error (RMSE) between the recovered and generative MLR parameters. The bottom panel of Fig. 2D shows that RMSE decreases fastest for infomax learning with Gibbs sampling in 2-d. Finally, Figure 2E shows that in the space of 10-d inputs, RMSE decreases fastest for infomax with Gibbs sampling, followed by infomax with variational inference (VI). This shows that sampling from the true posterior (with Gibbs sampling) leads to substantially better input selection, as compared to sampling from the variational posterior. Further, while DAD is comparable to infomax with VI in 2-d, it is not well suited for high-dimensional inputs. Given that RMSE is *not* the objective function we directly optimize with infomax, these results are particularly exciting. Overall, they suggest that our active learning method is sample-efficient in training MLRs.

As discussed earlier, in case of 2-d, this is because the Fisher Information drops dramatically when the angle between the weight vectors and the input is close to 90° or 270° . Hence, our active learning strategy outperforms random sampling by avoiding the uninformative inputs orthogonal to the model weights. In S5, we verify that our approach does avoid these inputs and show a histogram of the selected inputs for the experiments of Fig. 2D. Further, as the Fisher information analysis given above makes clear, higher dimensionality leads to increased probability that randomly selected inputs will fall in the region of non-identifiability, given that random vectors in high dimensions have high probability of being orthogonal [29]. This aligns with our finding that the benefits of active learning are more pronounced in higher dimensions.

Application: CA Housing Dataset

Finally, we applied infomax learning to the California housing dataset of [33]. This dataset contains the median house price, in 1990, as well as 8 predictors of house price for 20,640 census block groups. The dataset is accessible via scikit-learn [50].

We fit MLRs with different numbers of states to a reduced dataset of 5000 samples and found that a 3 state MLR described the CA housing dataset well (Figure 3C), and offered a dramatic improvement in predictive power relative to standard linear regression (a 1 state MLR). Figures 3A and 3B show the best fitting mixing weights and state weights for this 3 state MLR. Next, we wanted to understand if infomax learning would allow us to learn the best-fitting 3 state MLR parameters with fewer samples. We use infomax with Gibbs sampling, and in Figures 3D and 3E show that infomax learning does, indeed, significantly reduce the number of samples required to learn the model parameters.

In Figure 3B, it is clear that the three states differ most according to the weights placed on the ‘AveOccup’ (average occupancy), ‘Latitude’ and ‘Longitude’ covariates. Intriguingly, in Figure 3F, we see that the inputs selected by infomax always have greater variance for the Latitude and Longitude covariates compared to those selected with random sampling (the red crosses are always

above the blue dots). This is a useful external validation that infomax selects inputs in a sensible way.

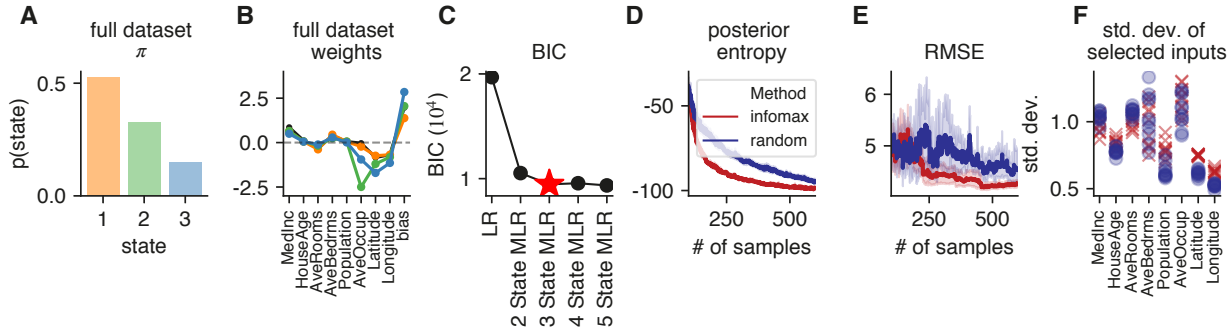


Figure 3: Application of infomax learning to California Housing Dataset [33]. **(A)** Best fitting mixing weights for 3 state MLR to 5000 samples of the CA housing dataset. **(B)** Best fitting state weights for 3 state MLR to 5000 samples of the CA housing dataset. Orange, green and blue represent states 1, 2 and 3 respectively. Black represents the linear regression fit to the same dataset. **(C)** BIC as number of MLR states is varied from 1 (standard linear regression) to 5. We focus on the 3 state model as BIC begins to level off beyond 3 states. **(D)** Posterior entropy between the 3 state MLR parameters obtained using 5000 samples (parameters shown in (A) and (B)) and recovered parameters as a function of the number of samples for random sampling (blue) and infomax with gibbs sampling (red). Error bars reflect 95% confidence interval of the mean across 10 experiments. **(E)** The same as in (D) but for the RMSE (root mean squared error). **(F)** Visualization of standard deviation of 500 inputs selected by both infomax (red) and random sampling (blue). Each dot corresponds to a different experiment. Examining (B), it is clear that the 3 states differ most according to the weights placed on the ‘AveOccup’, ‘Latitude’ and ‘Longitude’ covariates. Intriguingly, we see that all 10 infomax experiments select inputs with greater variance for the latitude and longitude covariates than are selected by the random sampling experiments.

5 Input-Output Hidden Markov Models

Input-Output Hidden Markov Models (IO-HMMs) [6] are extensions of standard HMMs. A standard HMM has K discrete states and at each time step t the observed output, y_t , depends only on the current state, $z_t \in \{1, \dots, K\}$. The states themselves have Markovian transitions between them. As shown in Fig. 4A, IO-HMMs have an additional component: an external input is presented at every time step, $\mathbf{x}_t \in \mathbb{R}^D$. As a result, state transitions and observations can be conditioned on the input at the current time step. Also known as GLM-HMMs in the neuroscience literature [2, 9, 10, 19], these models allow transitions and observations to be generated by state-dependent generalized linear models (GLMs).

Here, we consider the Bernoulli IO-HMM, which assumes that the outputs are binary, $y_t \in \{0, 1\}$, and are produced according to state-specific GLM weights, $\mathbf{w}_k \in \mathbb{R}^D$:

$$p(y_t = 1 \mid \mathbf{x}_t, z_t = k) = \frac{1}{1 + \exp^{-\mathbf{w}_k^\top \mathbf{x}_t}} \quad (6)$$

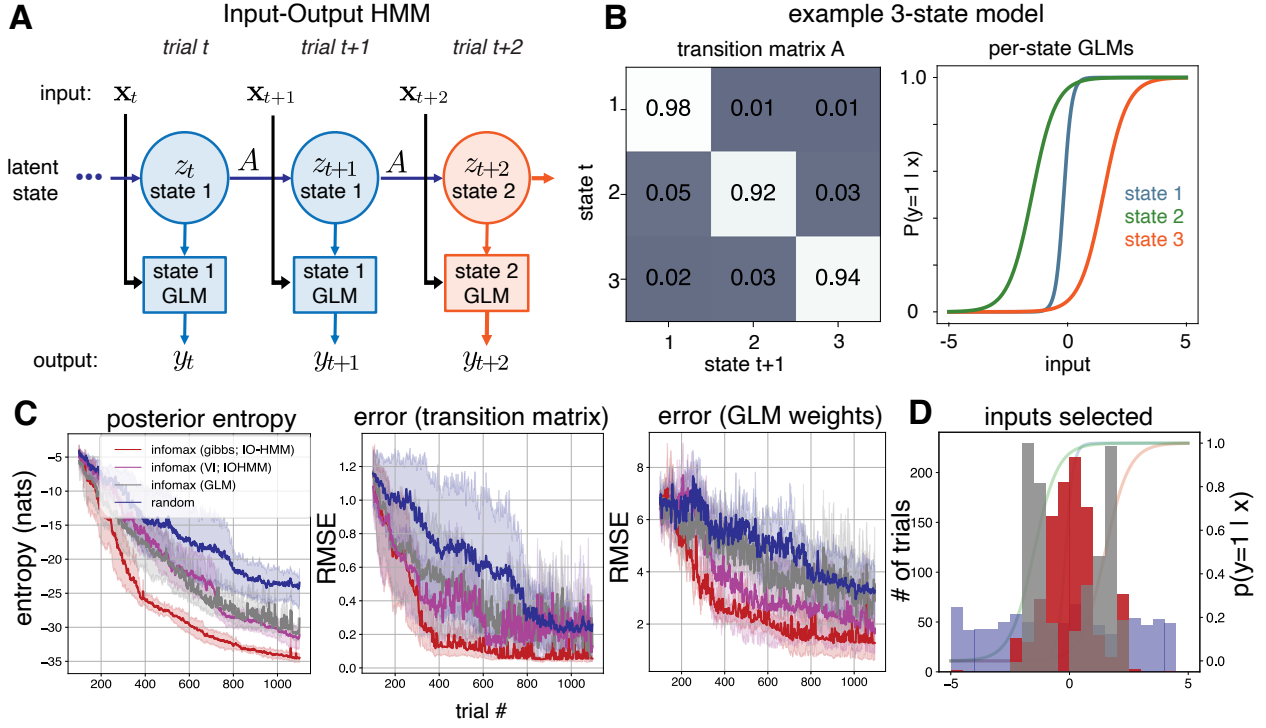


Figure 4: Infomax for IO-HMMs. (A) Data generation process for the IO-HMM. At time step t , a system generates output y_t based on its input, \mathbf{x}_t , as well as its latent state at that time step, z_t . The system then either remains in the same state, or transitions into a new state at trial $t + 1$, with the transition probabilities given by matrix A . (B) Example settings for the transition matrix and state GLMs for a 3 state IO-HMM. These are the settings we use to generate output data for the analyses shown in panels C and D. (C) Left: posterior entropy over the course of 1000 trials for random sampling (blue), infomax with a single GLM (grey), infomax for the full IO-HMM using variational inference (VI) and Gibbs sampling (magenta and red respectively). Middle: root mean squared error for the recovered transition matrix for each of the three input-selection schemes (random/infomax with GLM/infomax with IO-HMM (Gibbs)/infomax with IO-HMM (VI)). Right: root mean squared error for the weight vectors of the IO-HMM for each of the input-selection schemes. (D) Selected inputs for random sampling (blue), active learning when there is model mismatch and the model used for infomax is a single GLM (gray), active learning with infomax (using Gibbs sampling) and the full IO-HMM (red). Selected inputs over the course of 1000 trials are plotted, and are shown on top of the generative GLM curves.

We assume that, as in the standard HMM, state transitions are governed by a stationary, input-independent transition matrix, $A \in \mathbb{R}^{K \times K}$, where $A_{il} = p(z_t = l | z_{t-1} = i)$. The first state z_1 has prior distribution $\pi \in \Delta^{K-1}$.

To perform infomax learning with IO-HMMs, we first use Gibbs sampling to iteratively sample the latent states $z_{t'} \forall t' \in [1, t]$, and the model parameters $\{\mathbf{w}_{1:K}, A, \pi\}$, after each trial (step 2 in Fig. 1). Gibbs sampling-based inference for HMMs is well-known [26]. However, when we use Bernoulli-GLM observations, the conditional distribution over $\{\mathbf{w}_{1:K}\}$ is no longer available in closed form since the Bernoulli-GLM likelihood does not have a conjugate prior distribution. As a result, we came up with an alternative solution for sampling $\{\mathbf{w}_{1:K}\}$, using Laplace approximation,

which we detail in the supplement S7. An alternative strategy for sampling from logistic models involves using Polya-Gamma augmentation [51, 54]. We show in the supplement, S9, that our approach performs just as well as Polya-Gamma augmentation, thereby empirically validating our Laplace-based Gibbs sampler.

We also perform infomax learning using variational inference (VI). We use mean-field VI to obtain posterior distributions over the model parameters $\{\mathbf{w}_{1:K}, A, \pi\}$. Due to the absence of a conjugate prior for Bernoulli observations, the distribution over $\{\mathbf{w}_{1:K}\}$ is not available in closed form and so we resort to Laplace approximation for obtaining variational posteriors over the weights (see S8 for the full algorithm). Upon obtaining the distributions, we draw samples of model parameters from their variational posteriors.

During infomax learning with IO-HMMs (step 3 of Fig. 1), we use M samples of the model parameters, $\{\mathbf{w}_{1:K}^j, A^j, \pi^j\}_{j=1}^M$, to compute the mutual information between the output and the model parameters according to Eq. 3. Here, the likelihood for the IO-HMM is:

$$p(y | \theta^j, x, \mathcal{D}_t) = \sum_{k=1}^K p(z = k | \mathcal{D}_t, \theta^j) p(y | x, z = k) \quad (7)$$

where $p(z = k | \mathcal{D}_t, \theta^j)$ can readily be obtained using the forward-backward algorithm and $p(y | x, z = k)$ is the Bernoulli-GLM likelihood function (Eq. 6). After computing the mutual information, we optimize it over a discrete set of inputs to find the next input to present to the system.

Experiments with IO-HMMs

We generate data from the 3-state IO-HMM shown in Fig. 4B. We set the parameters to match those in [2], which fit the IO-HMM to the binary choice data of mice performing a decision-making experiment. Each GLM has a weight associated with the external stimulus (w_k) presented to the mouse, as well as a bias parameter (b_k), such that $\mathbf{w}_k = \{w_k, b_k\}$. The input stimuli (x_t) are 1-dimensional, such that the choice probability can be formally written as:

$$p(y_t = 1 | \mathbf{x}_t, z_t = k) = \frac{1}{1 + \exp^{-w_k x_t + b_k}} \quad (8)$$

In our experiment, we choose input stimuli such that they lie in $[-5, 5]$ and are 0.01 units apart. Similar to the MLR setting, the task here is to recover the generative parameters of the IO-HMM. We do this via our infomax learning methods (using Gibbs sampling as well as variational inference) as well as a random sampling approach where inputs are selected at random from the specified set; Deep Adaptive Design (DAD) [23] is not applicable in this setting as it assumes trials to be i.i.d. We find that the posterior entropy over the model parameters decreases dramatically faster using infomax learning with Gibbs sampling, followed by infomax with variational inference compared to random sampling (compare the red, magenta and blue curves in the left panel of Fig. 4C). We also observe that the RMSE between the generative and recovered parameters decreases much faster for our active learning methods (infomax using Gibbs, followed by infomax using variational inference) as compared to random sampling for the transition matrix A (middle panel of Fig. 4C), as well as for the GLM weights (right panel of Fig. 4C). This suggests that our infomax learning method can be used to fit IO-HMMs using fewer samples; and reinforces our previous result that sampling from the exact posterior substantially benefits infomax learning as compared to using the variational posterior.

Finally, to understand why our active learning framework outperforms random sampling for the IO-HMM, we plot histograms of the inputs selected by random sampling and by infomax learning using Gibbs sampling (Fig. 4D). While random sampling selects inputs from the entire input domain, infomax learning rarely selects inputs with a magnitude greater than 3. For positive inputs with a magnitude greater than 3, for all three models, the sigmoid of Eq. 8 saturates and all generated y_t values will be 1. Similarly, for large negative inputs, all generated y_t output values will be 0. As such, these large magnitude inputs generate outputs that provide no information either about the latent that generated the data (necessary for updating the transition matrix) or the weights used to generate the data. Overall, infomax learning reduces the number of samples required to learn the parameters of the IO-HMM.

To make our method practical for closed-loop experiments, it is critical that the method compute new inputs quickly. For example, in the case of mouse decision-making experiments, consecutive trials occur within 1–10 seconds [38, 53]. While our current implementation requires up to 20s per trial (on an 1.7GHz quad-core i7 laptop), we show in the supplement (S9) that running five parallel chains of 100 samples each provides a 5x speedup over the current implementation with a single chain of 500 Gibbs samples.

Additionally, we also perform infomax learning for a special case of IO-HMMs: mixtures of GLMs. We show in S10 that our method outperforms random sampling in terms of posterior entropy and error in recovering the model parameters. These results provide further evidence that our infomax learning method is applicable across model settings.

Consequences of ignoring latent states

To assess the importance of latent structure on active learning methods, we benchmarked our method against an additional input-selection scheme: infomax under conditions of model mismatch. Specifically, we compared to a strategy where inputs were selected by infomax under the (mismatched) assumption that responses arose from a single Bernoulli-GLM, with no latent states. This allowed us to explore the effect of ignoring the presence of latent variables when selecting inputs.

Fig. 4D shows that the inputs selected by Bernoulli-GLM infomax learning differed substantially from those selected by the full IO-HMM infomax algorithm. In particular, the Bernoulli-GLM method avoided selecting inputs in both the center and the outer edges of the input domain. In virtue of neglecting the outer edges, it outperformed random input selection (compare the grey and blue lines in all panels of Fig. 4C). However, the full IO-HMM infomax method still performed best for learning the weights and transition matrix of the true model (red lines in Fig. 4C). The significant drop in the performance when ignoring the presence of latent states thus highlights the importance of developing active learning methods tailored specifically for latent variable models.

Downstream application: latent state inference

IO-HMMs are often used to infer the underlying latent states during the course of an experiment. To demonstrate the utility of our active learning approach for downstream tasks, we compare infomax learning and random sampling for predicting latent states across trials. We use the same generative IO-HMM as shown in Fig. 4B, and train two new distinct IO-HMMs using 400 input-output samples from the generative model. One of the IO-HMMs is trained using inputs selected by infomax learning (with Gibbs sampling), while the other is trained using random input selection. Next, we generate a set of 100 trials from the generative model, and use the two IO-HMMs to predict the posterior

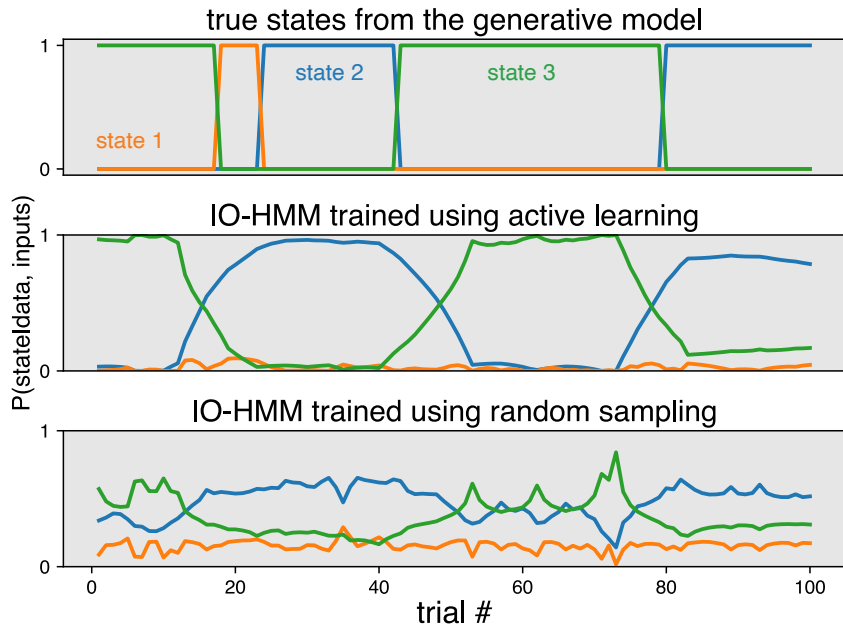


Figure 5: Inferring latent states. (Top) the true latent states of the data-generating IO-HMM for 100 trials. (Middle) the inferred posterior probabilities of states using an IO-HMM, trained using infomax learning on 400 trials from the data-generating IO-HMM. (Bottom) the same for an IO-HMM trained using random sampling on 400 trials from the data-generating IO-HMM. probabilities of states as each trial. Fig. 5 shows that the IO-HMM trained using infomax learning is able to predict the true states drastically better than that trained using random selection using the same number of trials.

6 Discussion

We developed a novel method to perform Bayesian active learning for discrete latent variable models. We applied this method to two distinct classes of latent variable models: mixture of linear regressions (MLRs) and input-output HMMs (IO-HMMs). We showed that, in both cases, infomax learning consistently achieved lower error and lower posterior entropy than random input selection. Our method also outperformed active learning methods that ignored the presence of latent variables and, for the case of MLRs, the Deep Active Design method of [23].

Given the importance of latent variable modeling in neuroscience [2, 9, 10, 19] as well as in other scientific domains [7], we envisage broad applicability of our method. One exciting application involves using our method to adaptively select stimuli in animal decision-making tasks. Recent work has shown that the behavior of mice can be well-described with a multi-state IO-HMM [2]. One limitation of that work, however, is that it required large amounts of data, collected from multiple sessions across multiple days, to learn the IO-HMM parameters. Using our framework, it may be possible to learn these parameters using data from only a single day, reducing the time and cost of experiments and thereby speeding up scientific discovery.

Nevertheless, there are several limitations of our current work. First, we considered the output observations y to be scalar. Extending to higher-dimensional outputs may require alternate methods for computing information, given the difficulty of numerical integration in high dimensions. Second,

in the experiments presented here, we selected maximally informative inputs from a discrete set of candidate inputs on each trial. Future work may instead use optimization to find optimal inputs in a continuous input space. A final direction for future work is to consider IO-HMMs in which state transitions also dependent on the input. Despite these limitations, our method achieves substantial advances for the learning of systems characterized by latent variable models, and we feel it will be highly beneficial in neuroscience and other fields where experiments are time-consuming or expensive.

References

- [1] Anderson, B. and Moore, A. (2005). Active learning for hidden markov models: Objective functions and algorithms. In *Proceedings of the 22nd International Conference on Machine Learning*, ICML '05, page 9–16. Association for Computing Machinery.
- [2] Ashwood, Z. C., Roy, N. A., Stone, I. R., Laboratory, T. I. B., Churchland, A. K., Pouget, A., and Pillow, J. W. (2021). Mice alternate between discrete strategies during perceptual decision-making. *bioRxiv*, page 2020.10.19.346353. Publisher: Cold Spring Harbor Laboratory.
- [3] Bak, J. H., Choi, J., Witten, I., Akrami, A., and Pillow, J. W. (2016). Adaptive optimal training of animal behavior. In *NIPS*, pages 1939–1947.
- [4] Bak, J. H. and Pillow, J. W. (2018). Adaptive stimulus selection for multi-alternative psychometric functions with lapses. *Journal of Vision*, 18(12):4.
- [5] Behboodian, J. (1972). Information matrix for a mixture of two normal distributions. *Journal of statistical computation and simulation*, 1(4):295–314.
- [6] Bengio, Y. and Frasconi, P. (1995). An Input Output HMM Architecture. In Tesauro, G., Touretzky, D. S., and Leen, T. K., editors, *Advances in Neural Information Processing Systems 7*, pages 427–434. MIT Press.
- [7] Bishop, C. M. (2006). *Pattern Recognition and Machine Learning*. Springer.
- [8] Blei, D. M., Kucukelbir, A., and McAuliffe, J. D. (2017). Variational inference: A review for statisticians. *Journal of the American Statistical Association*, 112(518):859–877.
- [9] Bolkan, S. S., Stone, I. R., Pinto, L., Ashwood, Z. C., Iravedra Garcia, J. M., Herman, A. L., Singh, P., Bandi, A., Cox, J., Zimmerman, C. A., Cho, J. R., Engelhard, B., Pillow, J. W., and Witten, I. B. (2022). Opponent control of behavior by dorsomedial striatal pathways depends on task demands and internal state. *bioRxiv*, page 2021.07.23.453573.
- [10] Calhoun, A. J., Pillow, J. W., and Murthy, M. (2019). Unsupervised identification of the internal states that shape natural behavior. *Nature Neuroscience*, 22(12):2040–2049. Number: 12 Publisher: Nature Publishing Group.
- [11] Chaloner, K. et al. (1984). Optimal bayesian experimental design for linear models. *The Annals of Statistics*, 12(1):283–300.
- [12] Chaloner, K. and Verdinelli, I. (1995). Bayesian Experimental Design: A Review. *Statistical Science*, 10(3):273–304. Publisher: Institute of Mathematical Statistics.

- [13] Chen, Z., Vijayan, S., Barbieri, R., Wilson, M. A., and Brown, E. N. (2009). Discrete- and continuous-time probabilistic models and algorithms for inferring neuronal up and down states. *Neural Computation*, 21(7):1797–1862. PMID: 19323637.
- [14] Cohn, D. A., Ghahramani, Z., and Jordan, M. I. (1996). Active Learning with Statistical Models. *Journal of Artificial Intelligence Research*, 4:129–145.
- [15] Cowley, B., Williamson, R., Clemens, K., Smith, M., and Byron, M. Y. (2017). Adaptive stimulus selection for optimizing neural population responses. In *Advances in Neural Information Processing Systems*, pages 1395–1405.
- [16] DiMattina, C. (2015). Fast adaptive estimation of multidimensional psychometric functions. *Journal of Vision*, 15(9):5–5.
- [17] DiMattina, C. and Zhang, K. (2011). Active data collection for efficient estimation and comparison of nonlinear neural models. *Neural computation*, 23(9):2242–2288.
- [18] DiMattina, C. and Zhang, K. (2013). Adaptive stimulus optimization for sensory systems neuroscience. *Frontiers in neural circuits*, 7.
- [19] Escola, S., Fontanini, A., Katz, D., and Paninski, L. (2011). Hidden Markov models for the stimulus-response relationships of multistate neural systems. *Neural Computation*, 23(5):1071–1132.
- [20] Farewell, V. T. and Sprott, D. A. (1988). The Use of a Mixture Model in the Analysis of Count Data. *Biometrics*, 44(4):1191–1194. Publisher: [Wiley, International Biometric Society].
- [21] Follmann, D. A. and Lambert, D. (1989). Generalizing logistic regression by nonparametric mixing. *Journal of the American Statistical Association*, 84(405):295–300. Publisher: Taylor & Francis Group.
- [22] Follmann, D. A. and Lambert, D. (1991). Identifiability of finite mixtures of logistic regression models. *Journal of Statistical Planning and Inference*, 27(3):375–381. Publisher: Elsevier.
- [23] Foster, A., Ivanova, D. R., Malik, I., and Rainforth, T. (2021). Deep Adaptive Design: Amortizing Sequential Bayesian Experimental Design. In *Proceedings of the 38th International Conference on Machine Learning*, pages 3384–3395. PMLR. ISSN: 2640-3498.
- [24] Gaffney, S. and Smyth, P. (1999). Trajectory clustering with mixtures of regression models. In *Proceedings of the fifth ACM SIGKDD international conference on Knowledge discovery and data mining*, pages 63–72.
- [25] Gal, Y., Islam, R., and Ghahramani, Z. (2017). Deep Bayesian Active Learning with Image Data. *arXiv:1703.02910 [cs, stat]*. arXiv: 1703.02910.
- [26] Ghahramani, Z. (2001). An introduction to hidden markov models and bayesian networks. *IJPRAI*, 15:9–42.
- [27] Glaser, J. I., Whiteway, M. R., Cunningham, J. P., Paninski, L., and Linderman, S. W. (2020). Recurrent switching dynamical systems models for multiple interacting neural populations. *bioRxiv*.
- [28] Gollisch, T. and Herz, A. V. (2012). The iso-response method: measuring neuronal stimulus integration with closed-loop experiments. *Frontiers in neural circuits*, 6.

- [29] Gorban, A. N. and Tyukin, I. Y. (2018). Blessing of dimensionality: mathematical foundations of the statistical physics of data. *Philosophical Transactions of the Royal Society A: Mathematical, Physical and Engineering Sciences*, 376(2118):20170237. arXiv: 1801.03421.
- [30] Hefang, L., Myers, R. H., and Keying, Y. (2000). Bayesian two-stage optimal design for mixture models. *Journal of Statistical Computation and Simulation*, 66(3):209–231.
- [31] Houlsby, N., Huszár, F., Ghahramani, Z., and Lengyel, M. (2011). Bayesian Active Learning for Classification and Preference Learning. *arXiv:1112.5745 [cs, stat]*. arXiv: 1112.5745.
- [32] Ivanova, D. R., Foster, A., Kleinegesse, S., Gutmann, M. U., and Rainforth, T. (2021). Implicit Deep Adaptive Design: Policy-Based Experimental Design without Likelihoods.
- [33] Kelley Pace, R. and Barry, R. (1997). Sparse spatial autoregressions. *Statistics & Probability Letters*, 33(3):291–297.
- [34] Khuri, A. I., Mukherjee, B., Sinha, B. K., and Ghosh, M. (2006). Design issues for generalized linear models: A review. *Statistical Science*, pages 376–399.
- [35] Kim, W., Pitt, M. A., Lu, Z.-L., Steyvers, M., and Myung, J. I. (2014). A hierarchical adaptive approach to optimal experimental design. *Neural Computation*, 26(11):2465–2492.
- [36] Kirsch, A., van Amersfoort, J., and Gal, Y. (2019). Batchbald: Efficient and diverse batch acquisition for deep bayesian active learning. In Wallach, H., Larochelle, H., Beygelzimer, A., Alché-Buc, F., Fox, E., and Garnett, R., editors, *Advances in Neural Information Processing Systems*, volume 32. Curran Associates, Inc.
- [37] Kleinegesse, S. and Gutmann, M. U. (2020). Bayesian Experimental Design for Implicit Models by Mutual Information Neural Estimation. In *Proceedings of the 37th International Conference on Machine Learning*, pages 5316–5326. PMLR. ISSN: 2640-3498.
- [38] Laboratory, T. I. B., Aguilon-Rodriguez, V., Angelaki, D. E., Bayer, H. M., Bonacchi, N., Carandini, M., Cazes, F., Chapuis, G. A., Churchland, A. K., Dan, Y., Dewitt, E. E., Faulkner, M., Forrest, H., Haetzel, L. M., Hausser, M., Hofer, S. B., Hu, F., Khanal, A., Krasniak, C. S., Laranjeira, I., Mainen, Z. F., Meijer, G. T., Miska, N. J., Mrsic-Flogel, T. D., Murakami, M., Noel, J.-P., Pan-Vazquez, A., Sanders, J. I., Socha, K. Z., Terry, R., Urai, A. E., Vergara, H. M., Wells, M. J., Wilson, C. J., Witten, I. B., Wool, L. E., and Zador, A. (2020). A standardized and reproducible method to measure decision-making in mice. *bioRxiv*, page 2020.01.17.909838.
- [39] Lewi, J., Butera, R., and Paninski, L. (2007). Efficient active learning with generalized linear models. In *Artificial Intelligence and Statistics*, pages 267–274. PMLR.
- [40] Lewi, J., Butera, R., and Paninski, L. (2009). Sequential optimal design of neurophysiology experiments. *Neural Computation*, 21(3):619–687.
- [41] Lewi, J., Schneider, D. M., Woolley, S. M. N., and Paninski, L. (2011). Automating the design of informative sequences of sensory stimuli. *J Comput Neurosci*, 30(1):181–200.
- [42] Li, G. (2018). Application of Finite Mixture of Logistic Regression for Heterogeneous Merging Behavior Analysis. *Journal of Advanced Transportation*, 2018:e1436521. Publisher: Hindawi.
- [43] Li, Y. and Liang, Y. (2018). Learning mixtures of linear regressions with nearly optimal complexity. In *Conference On Learning Theory*, pages 1125–1144. PMLR.

- [44] Linderman, S. W., Johnson, M. J., Wilson, M. A., and Chen, Z. (2016). A bayesian non-parametric approach for uncovering rat hippocampal population codes during spatial navigation. *Journal of neuroscience methods*, 263:36–47.
- [45] Loredo, T. J. (2004). Bayesian Adaptive Exploration. *AIP Conference Proceedings*, 707(1):330–346. Publisher: American Institute of Physics.
- [46] MacKay, D. J. C. (1992). Information-Based Objective Functions for Active Data Selection. *Neural Computation*, 4(4):590–604.
- [47] Myung, J. I., Cavagnaro, D. R., and Pitt, M. A. (2013). A Tutorial on Adaptive Design Optimization. *Journal of mathematical psychology*, 57(3-4):53–67.
- [48] Paninski, L. (2005). Asymptotic theory of information-theoretic experimental design. *Neural Computation*, 17(7):1480–1507. Publisher: MIT Press.
- [49] Park, M., Weller, J. P., Horwitz, G. D., and Pillow, J. W. (2014). Bayesian active learning of neural firing rate maps with transformed gaussian process priors. *Neural Computation*, 26(8):1519–1541.
- [50] Pedregosa, F., Varoquaux, G., Gramfort, A., Michel, V., Thirion, B., Grisel, O., Blondel, M., Prettenhofer, P., Weiss, R., Dubourg, V., Vanderplas, J., Passos, A., Cournapeau, D., Brucher, M., Perrot, M., and Duchesnay, E. (2011). Scikit-learn: Machine learning in Python. *Journal of Machine Learning Research*, 12:2825–2830.
- [51] Pillow, J. and Scott, J. (2012). Fully Bayesian inference for neural models with negative-binomial spiking. In *Advances in Neural Information Processing Systems*, volume 25. Curran Associates, Inc.
- [52] Pillow, J. W. and Park, M. (2016). Adaptive bayesian methods for closed-loop neurophysiology. In El Hady, A., editor, *Closed Loop Neuroscience*, pages 3–18. Elsevier.
- [53] Pinto, L., Koay, S. A., Engelhard, B., Yoon, A. M., Deverett, B., Thiberge, S. Y., Witten, I. B., Tank, D. W., and Brody, C. D. (2018). An Accumulation-of-Evidence Task Using Visual Pulses for Mice Navigating in Virtual Reality. *Frontiers in Behavioral Neuroscience*, 12. Publisher: Frontiers.
- [54] Polson, N. G., Scott, J. G., and Windle, J. (2013). Bayesian inference for logistic models using pólya–gamma latent variables. *Journal of the American Statistical Association*, 108(504):1339–1349.
- [55] Roy, N. and McCallum, A. (2001). Toward optimal active learning through monte carlo estimation of error reduction. *ICML*, pages 441–448.
- [56] Settles, B. (2009). Active learning literature survey. Computer Sciences Technical Report 1648, University of Wisconsin–Madison.
- [57] Shababo, B., Paige, B., Pakman, A., and Paninski, L. (2013). Bayesian Inference and Online Experimental Design for Mapping Neural Microcircuits. In *NIPS*, volume 26, pages 1304–1312.
- [58] Steinke, F., Seeger, M., and Tsuda, K. (2007). Experimental design for efficient identification of gene regulatory networks using sparse bayesian models. *BMC Systems Biology*, 1(1):51.

- [59] Verdinelli, I. and Kadane, J. B. (1992). Bayesian designs for maximizing information and outcome. *J. Amer. Statist. Assoc.*, 87(418):510–515.
- [60] Watson, A. and Pelli, D. (1983). QUEST: a Bayesian adaptive psychophysical method. *Perception and Psychophysics*, 33:113–120.
- [61] Watson, A. B. (2017). Quest+: A general multidimensional bayesian adaptive psychometric method. *Journal of Vision*, 17(3):10.
- [62] Wedel, M. and DeSarbo, W. S. (1995). A mixture likelihood approach for generalized linear models. *Journal of classification*, 12(1):21–55. Publisher: Springer.
- [63] Wiltschko, A. B., Johnson, M. J., Iurilli, G., Peterson, R. E., Katon, J. M., Pashkovski, S. L., Abaira, V. E., Adams, R. P., and Datta, S. R. (2015). Mapping sub-second structure in mouse behavior. *Neuron*, 88(6):1121–1135.
- [64] Yu, B. M., Cunningham, J. P., Santhanam, G., Ryu, S. I., Shenoy, K. V., and Sahani, M. (2009). Gaussian-process factor analysis for low-dimensional single-trial analysis of neural population activity. *Journal of Neurophysiology*, 102(1):614.
- [65] Zoltowski, D. M., Pillow, J. W., and Linderman, S. W. (2020). A general recurrent state space framework for modeling neural dynamics during decision-making. In III, H. D. and Singh, A., editors, *Proceedings of the 37th International Conference on Machine Learning*, volume 119 of *Proceedings of Machine Learning Research*, pages 11680–11691, Virtual. PMLR.

A Appendix

S1 Infomax Learning using samples

Infomax entails computing the input, x , which maximizes the conditional mutual information between the outputs, y and model parameters, θ . One way to write mutual information is as follows:

$$I(\theta; y | \mathbf{x}, \mathcal{D}_t) = H(y; \mathbf{x}, \mathcal{D}_t) - H(y | \theta; \mathbf{x}, \mathcal{D}_t), \quad (\text{S1})$$

Since we follow a sampling-based strategy to compute the best input: $x = \max_x I(\theta; y | \mathbf{x}, \mathcal{D}_t)$, we can use the samples $\{\theta^j\}_{j=1}^M$ drawn from $p(\theta | \mathcal{D}_t)$ to approximate eq. S1. Each sample, θ^j , leads to a model-based likelihood $p(y | \theta^j, \mathbf{x}, \mathcal{D}_t)$. We can then compute the marginal likelihood:

$$p(y | \mathbf{x}, \mathcal{D}_t) \approx \frac{1}{M} \sum_{j=1}^M p(y | \theta^j, \mathbf{x}, \mathcal{D}_t) \quad (\text{S2})$$

This results in sample-based versions of the entropy terms such that:

$$H(y | \theta; \mathbf{x}, \mathcal{D}_t) \approx \frac{1}{M} \sum_{j=1}^M \int p(y | \theta^j, \mathbf{x}, \mathcal{D}_t) \log p(y | \theta^j, \mathbf{x}, \mathcal{D}_t) dy \quad (\text{S3})$$

$$H(y; \mathbf{x}, \mathcal{D}_t) = \int p(y | \mathbf{x}, \mathcal{D}_t) \log p(y | \mathbf{x}, \mathcal{D}_t) dy \quad (\text{S4})$$

$$\approx \int \left(\frac{1}{M} \sum_{j=1}^M p(y | \theta^j, \mathbf{x}, \mathcal{D}_t) \right) \log \left(\frac{1}{M} \sum_{j=1}^M p(y | \theta^j, \mathbf{x}, \mathcal{D}_t) \right) dy \quad (\text{S5})$$

Substituting these into the mutual information (eq. S1) results in the sample-based form of mutual information that we use in our experiments:

$$I(\theta; y | \mathbf{x}, \mathcal{D}_t) \approx \frac{1}{M} \sum_{j=1}^M D_{KL} (p(y | \theta^j, \mathbf{x}, \mathcal{D}_t) || p(y | \mathbf{x}, \mathcal{D}_t)) \quad (\text{S6})$$

S2 Gibbs Sampling for MLRs

Here, we describe Gibbs Sampling algorithm for Mixture of Linear Regressions models. Given T trials, for each input-output pair, $\mathbf{x}_t \in \mathbb{R}^D$ and $y_t \in \mathbb{R}$, we sample class-belongings, $z_t \in \{1, \dots, K\}$, from:

$$p(z_t = k | y_t, \mathbf{x}_t, \mathbf{w}_{1:K}, \pi, \sigma) = \frac{\mathcal{N}(y_t; \mathbf{w}_k^\top \mathbf{x}_t, \sigma^2) \pi_k}{\sum_l \mathcal{N}(y_t; \mathbf{w}_l^\top \mathbf{x}_t, \sigma^2) \pi_l} \quad (\text{S7})$$

Next, we sample new estimates of the mixing parameters from:

$$\pi_k | z_{1:T} \sim \text{Dir}(n_k + 1) \quad (\text{S8})$$

where $n_k = \sum_{t'=1}^T \mathbb{1}(z_{t'} = k)$.

Finally, we assume a Gaussian prior, $\mathcal{N}(\mathbf{w}_0, \sigma_0^2 I)$, over the weights associated with each latent class and sample a new estimate for them as follows:

$$\mathbf{w}_k \sim \mathcal{N}(\mathbf{w}'_k, \Sigma'_k) \quad (\text{S9})$$

$$\mathbf{w}'_k = \mathbf{w}_0 + (\sigma_0^2 I + X_k X_k^\top)^{-1} X_k^\top (Y_k - X_k \mathbf{w}_0) \quad (\text{S10})$$

$$\Sigma'_k = I - X_k^\top \left(\sigma_0^2 I + X_k X_k^\top \right)^{-1} X_k. \quad (\text{S11})$$

Here, the rows of $X_k \in T_k \times D$ and $Y_k \in T_k \times 1$ contain inputs and outputs at time points where $z = k$, respectively. We fix $\mathbf{w}_0 = \mathbf{0}$ and $\sigma_0^2 = 10$ in our experiments. We perform this procedure M times in order to obtain M samples of the model parameters, $\{\mathbf{w}_{1:K}^j, \pi^j\}_{j=1}^M$, where $M = 500$ (excluding 100 burn-in samples) in our experiments.

S3 Variational inference for MLRs

Here, we describe mean-field variational inference for MLRs, which we use to derive posterior distributions over the model’s parameters. Following mean-field approximation, we assume independence between all the model parameters and the latent variables.

Given T trials, for each input-output pair, $\mathbf{x}_t \in \mathbb{R}^D$ and $y_t \in \mathbb{R}$, we assume that it’s mixture assignment $z_t \in \{1, \dots, K\}$ is governed by an independent categorical distribution $q(z_t; \phi_t)$, where $\phi_t \in \Delta^{K-1}$. We, further, assume that the weight $\mathbf{w}_k \in \mathbb{R}^D$ of the k -th linear regression model has a normal posterior distribution $q(\mathbf{w}_k; \mu_k, \Sigma_k)$, with mean $\mu_k \in \mathbb{R}^D$ and covariance $\Sigma_k \in \mathbb{R}^{D \times D}$. Hence:

$$q(\mathbf{w}_{1:K}, z_{1:T}) = \prod_{t=1}^T q(z_t; \phi_t) \prod_{k=1}^K q(\mathbf{w}_k; \mu_k, \Sigma_k) \quad (\text{S12})$$

Let us vertically stack ϕ_t for $t \in 1 : T$ and denote this by a matrix ϕ if size $T \times K$. Similarly, let $X \in \mathbb{R}^{T \times D}$ represent the design matrix with all inputs stacked, and $Y \in \mathbb{R}^{T \times 1}$ contain all observations. Also, we know that each of the linear regressions in the MLR model has Gaussian noise with variance σ^2 .

We update the variational parameters ϕ_t , $\mu_{1:K}$ and $\Sigma_{1:K}$ iteratively using the update rules described below. For each $t \in \{1..T\}$,

$$\phi_{tk} \propto \exp\{y_t x_t^\top \mathbb{E}[\mu_k] - \mathbb{E}[(x_t^\top \mu_k)^2]/2\} \quad (\text{S13})$$

Next, for each $k \in \{1..K\}$, we assume a Gaussian prior distribution over the weights: $\mathcal{N}(\mathbf{w}_0, \sigma_0^2 I)$, we update the variational parameters governing the weights as follows:

$$\Sigma_k = \left(\sigma_0^2 I + \frac{1}{\sigma^2} ((\phi_{:,k} \mathbf{1}) \cdot X)^\top X \right)^{-1} \quad (\text{S14})$$

$$\mu_k = \frac{1}{\sigma^2} \Sigma_k X^\top (\phi_{:,k} Y) \quad (\text{S15})$$

We fix $\mathbf{w}_0 = \mathbf{0}$ and $\sigma^2 = 10$ in our experiments. We repeat these updates until either the log-likelihood of the data arising from the model has converged or a limit of 500 iterations has reached.

Once the variational posteriors have been learned, we draw M samples each, for the weights $\mathbf{w}_{1:K}$ and the mixture assignments $z_{1:T}$. Finally, using the mixture assignments, we obtain M samples for the mixing probability π by computing the proportion of trials assigned to each state. We set $M = 500$ in our experiments, thus obtaining $\{\mathbf{w}_{1:K}^j, \pi^j\}_{j=1}^{500}$.

S4 Training details for Deep Adaptive Design (DAD)

We downloaded the code for DAD, and adapted it to perform input selection for MLRs (which we attach with the supplement). The parameters of the MLR model were set to the same values as described in sec. 4. Since the DAD model requires continuous inputs, rather than a discrete list of inputs, we allow it to choose inputs from the unit circle in 2d and the unit hypersphere in 10d, rather than restricting it to the discrete set of stimuli in sec. 4.

The DAD model has two components: the encoder network which takes in input-observation pairs $\{x, y\}$ and outputs an encoding for this. This is a feedforward neural network. We set this network to have 3 layers: the input layer which has 3 nodes for the first MLR experiment (2d inputs and 1d observations) and 11 nodes for the second experiment (10-d inputs and 1d observations), a hidden layer with 256 nodes and ReLu activation function, and a linear output layer with 16 nodes.

Following this, the encoded history is taken as input by an emitter network. This network outputs the input for the next trial: x_t . The input layer of this feedforward network has the same dimensionality as the output of the embedding layer, i.e. 16 nodes. It has one hidden layer with ReLu activation and 256 nodes, followed by a linear output layer with as many nodes as the dimensionality of the input to the MLR model. We normalize the output of this network, to ensure that the selected x_t lies on the unit circle/unit hypersphere.

We do a hyperparameter optimization to select the number of hidden layers and nodes from the range of values used in the experiments (no. of hidden layers: 1–3, no. of nodes per layer: 16/128/256) in the original DAD [23] paper.

To compute the sPCE loss that DAD uses to optimize the two neural networks, we use 500 samples each to compute the inner and outer expectation in the loss function. Since our experiments involve large number of trials ($T = 200$), we use score gradient estimator to compute the gradients that are backpropagated while training. Finally, we train the model using Adam (with betas set to 0.8, 0.998), and use exponential learning rate annealing (where the initial learning rate is set to $1e-4$ post a search over the range $1e-5$ – $1e-3$, and $\gamma = 0.96$) for a total of 50000 gradient steps.

S5 Inputs selected during active learning for MLRs

Fig. S1 shows the inputs selected by infomax learning and Deep Adaptive Design (DAD) on mixture of linear regressions.

S6 Fisher Information for MLRs

Here we derive the Fisher information for the weights of the MLR model (shown in Fig.2B of the main text).

We consider a model consisting of a mixture of K linear regression models in a D -dimensional input space, defined by weights $\{\mathbf{w}_1, \mathbf{w}_2, \dots, \mathbf{w}_K\}$. The full model weights take the form of a length- KD vector formed by stacking the weights for each component:

$$\mathbf{w} = \begin{bmatrix} \mathbf{w}_1 \\ \vdots \\ \mathbf{w}_K \end{bmatrix}. \tag{S16}$$

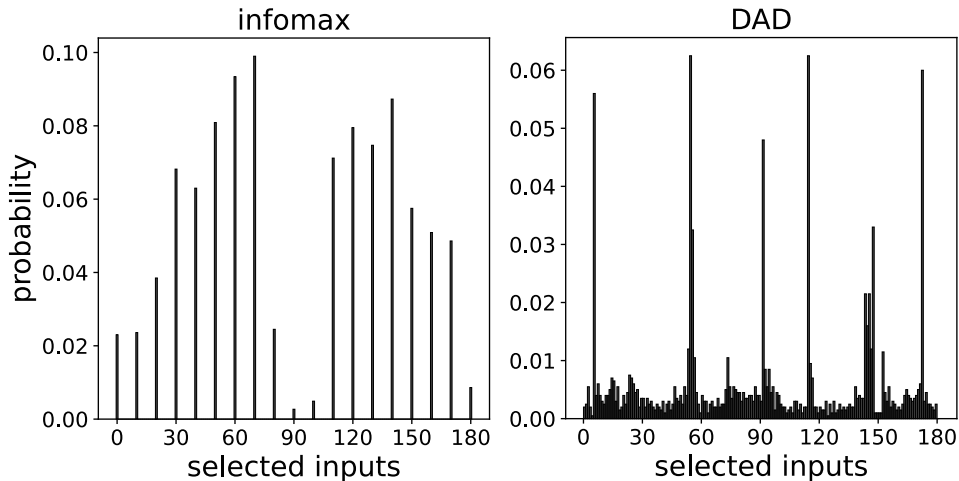


Figure S1: Histogram showing inputs selected by our active learning method (over the course of 200 trials) on mixture of linear regressions (MLRs), when inputs lie on a 2D circle (see Fig. 2). We find a drop in probability at 90° , this is also predicted by the Fisher Information analysis discussed in text for infomax (using Gibbs sampling). However, we do not see such a trend while using DAD. Inputs here are randomly distributed over the unit circle, with modes at multiple of 30° . (DAD requires a continuous range of inputs, hence we let it select inputs from all over the unit circle as opposed to a discrete list, as in Fig. 2.)

The Fisher information J is a $KD \times KD$ matrix carrying the expectation for the product of partial derivatives of the log-likelihood with respect to each element of \mathbf{w} . We will derive the $D \times D$ blocks of the Fisher information matrix for each pair of components in $\{1, \dots, K\}$.

The block of partial derivatives for component j is given by:

$$\begin{aligned}
 \frac{\partial}{\partial \mathbf{w}_j} \log p(y | \mathbf{x}, \theta) &= \frac{1}{\sigma^2} (y - \mathbf{x}^\top \mathbf{w}_j) \mathbf{x} \left(\frac{\pi_j \exp(-\frac{1}{2\sigma^2} (y - \mathbf{x}^\top \mathbf{w}_j)^2)}{p(y | \mathbf{x}, \theta)} \right) \\
 &= \frac{1}{\sigma^2} (y - \mathbf{x}^\top \mathbf{w}_j) \mathbf{x} \left(\frac{P(y | \mathbf{x}, z = j, \theta) P(z = j | \pi)}{p(y | \mathbf{x}, \theta)} \right) \\
 &= \frac{1}{\sigma^2} (y - \mathbf{x}^\top \mathbf{w}_j) \mathbf{x} \left(p(z = j | y, \mathbf{x}, \theta) \right). \tag{S17}
 \end{aligned}$$

Plugging this into the formula for Fisher information, we obtain the following expression for the i, j 'th block of the Fisher information matrix:

$$J_{[i,j]}(\mathbf{x}) = \frac{1}{\sigma^4} \mathbb{E} \left[(y - \mathbf{x}^\top \mathbf{w}_i) (y - \mathbf{x}^\top \mathbf{w}_j) p(z = i | y, \mathbf{x}, \theta) p(z = j | y, \mathbf{x}, \theta) \right] \mathbf{x} \mathbf{x}^\top, \tag{S18}$$

where expectation is taken with respect to the marginal distribution $p(y | \mathbf{x}, \theta)$. This expectation cannot in general be computed in closed form (see [5]). However, we considered two special cases in the text where an analytic expression is available.

Perfect identifiability

First, the case of ‘‘perfect identifiability’’ arises when the conditional distributions $p(y | \mathbf{x}, z = j, \theta)$ are well-separated for the different classes of latent variable z , or equivalently, the posterior class

probabilities $P(z = j | y, \mathbf{x}, \theta)$ are effectively 0 or 1 for virtually all output values y . In practice, this arises for inputs \mathbf{x} such that the conditional means $\{\mathbf{x}^\top \mathbf{w}_1, \mathbf{x}^\top \mathbf{w}_2, \dots, \mathbf{x}^\top \mathbf{w}_K\}$ are well separated relative to the noise standard deviation σ (e.g., more than 2σ apart). In this case, the off-diagonal blocks of the Fisher information matrix are zero, since $P(z = i | y, \mathbf{x}, \theta)P(z = j | y, \mathbf{x}, \theta) \approx 0$ for $i \neq j$. The diagonal blocks, by contrast, can be computed in closed form:

$$\begin{aligned} J_{[j,j]}(\mathbf{x}) &= \frac{1}{\sigma^4} \mathbb{E} \left[(y - \mathbf{x}^\top \mathbf{w}_j)^2 p(z = j | y, \mathbf{x}, \theta)^2 \right] \mathbf{x} \mathbf{x}^\top \\ &= \frac{1}{\sigma^4} \left(\int_{-\infty}^{\infty} (y - \mathbf{x}^\top \mathbf{w}_j)^2 \pi_j \mathcal{N}(y | \mathbf{x}^\top \mathbf{w}_j, \sigma^2) dy \right) \mathbf{x} \mathbf{x}^\top \\ &= \frac{1}{\sigma^2} \pi_j \mathbf{x} \mathbf{x}^\top. \end{aligned} \tag{S19}$$

We can write the Fisher information matrix efficiently as:

$$J(\mathbf{x}) = \frac{1}{\sigma^2} \text{diag}(\pi) \otimes \mathbf{x} \mathbf{x}^\top, \tag{S20}$$

where \otimes denotes the Kronecker product. The trace of the Fisher information is

$$\text{Tr}[J] = \frac{1}{\sigma^2} \text{Tr}[\text{diag}(\pi)] \text{Tr}[\mathbf{x} \mathbf{x}^\top] = \frac{1}{\sigma^2} \mathbf{x}^\top \mathbf{x}, \tag{S21}$$

which is the trace of the Fisher information matrix in the standard linear-Gaussian regression model. This confirms—as one might expect—that in the case of perfect identifiability we have the same amount of Fisher information as in a model without latent variables.

Non-identifiability

Second, the case of “non-identifiability” arises when the conditional distributions $p(y | \mathbf{x}, z = j, \theta)$ are identical for the different classes of latent variable z , meaning the output y carries no information about the model component that generated it. This arises when the linear projection of \mathbf{x} onto all of the weight vectors is identical, $\mathbf{x}^\top \mathbf{w}_1 = \mathbf{x}^\top \mathbf{w}_2 = \dots = \mathbf{x}^\top \mathbf{w}_K$. This arises, for example, when the stimulus is orthogonal to all of the weight vectors, which occurs with high probability in high-dimensional settings.

In this case we can also compute the Fisher information in closed form. We obtain, for block i, j of the Fisher information matrix:

$$\begin{aligned} J_{[i,j]}(\mathbf{x}) &= \frac{1}{\sigma^4} \mathbb{E} \left[(y - \mathbf{x}^\top \mathbf{w}_i)^2 \pi_i \pi_j \right] \mathbf{x} \mathbf{x}^\top \\ &= \frac{1}{\sigma^2} \pi_i \pi_j \mathbf{x} \mathbf{x}^\top, \end{aligned} \tag{S22}$$

where we have used the fact that $\mathbf{x}^\top \mathbf{w}_i = \mathbf{x}^\top \mathbf{w}_j$ and that the product of posterior probabilities $p(z = i | y, \mathbf{x}, \theta) p(z = j | y, \mathbf{x}, \theta)$ is equal to the product of prior probabilities $\pi_i \pi_j$ in the setting where the output y carries no information about the latent z .

The Fisher information matrix can be written in Kronecker form:

$$J = \frac{1}{\sigma^2} (\pi \pi^\top) \otimes \mathbf{x} \mathbf{x}^\top, \tag{S23}$$

which has trace

$$\text{Tr}[J] = \frac{1}{\sigma^2} (\pi^\top \pi) \mathbf{x}^\top \mathbf{x}. \tag{S24}$$

This expression is minimal when the prior probabilities are all equal to $1/K$, in which case $\pi^\top \pi = 1/K$, giving $\text{Tr}[J] = \frac{1}{K\sigma^2} \mathbf{x}^\top \mathbf{x}$.

S7 Gibbs Sampling For IO-HMMs

We provide a complete description of Gibbs sampling for IO-HMMs in Algorithm 1. It uses outputs $y_{1:T}$ and inputs $\mathbf{x}_{1:T}$, along with the prior over model parameters to provide M samples of the latent states $\{z_{1:T}\}^j$ as well as of the model parameters $\{\mathbf{w}_{1:K}, A, \pi\}^j$. We assume the model has K distinct latent states. Sampling the latent states (Alg. 3) requires using backward messages, $B_{t,k} = p(y_{t+1:T} \mid x_{1:T}, z_t = k)$, which can be obtained using standard forward-backward algorithm [7]. To sample the weights of the GLMs per state, we use the Laplace approximation followed by an acceptance-rejection step detailed in Alg. 2. We fix the Dirichlet prior $\alpha \in \mathbb{R}^{K+1 \times K}$ over the rows of the transition matrix, A , and the initial state distribution, π to be a matrix of ones. The GLM weights have an identical prior: $\mathcal{N}(\mathbf{0}, 10)$. Further, we run Gibbs sampling for 500 iterations and discard the first 100.

Algorithm 1 IO-HMM Gibbs Sampling

- 1: **Input:** Observations $y_{1:T}$, Inputs $\mathbf{x}_{1:T}$, Prior hyperparameters: $\alpha, \mathbf{w}_0, \sigma_0$
- 2: **Output:** Samples $\{(z_{1:T}, \mathbf{w}_{1:K}, A, \pi)^{(j)}\}$
- 3: Initialize $z_{1:T}, \mathbf{w}_{1:K}, A, \pi$
- 4: **for** $j \leftarrow 1, \dots, M$ **do**
- 5: **for** $k \leftarrow 1, \dots, K$ **do**
- 6: $\mathbf{w}_k^j \leftarrow \text{GLMsampleposterior}(\{y_t, \mathbf{x}_t \mid z_t = k\}_{1:T}, \mathbf{w}_0, \sigma_0, \mathbf{w}_k^{j-1})$
- 7: $A_{k,:}^j \leftarrow \text{sample Dir}(\alpha_{k,:} + \mathbf{n}_{k,:})$ {where $n_{kl} = \sum_t \mathbf{I}(z_t = k, z_{t+1} = l)$ }
- 8: **end for**
- 9: $z_{1:T}^j \leftarrow \text{IOHMMsamplestate}(\pi, A, L)$ {s.t. $L_{t,k} = p(y_t \mid \mathbf{x}_t, \mathbf{w}_k)$ }
- 10: $\pi^j \leftarrow \text{sample Dir}(\alpha_{0,:} + \mathbb{I}_{z_1})$
- 11: **end for**

Algorithm 2 GLM sample weight from posterior

- 1: **Input:** Observations $y_{1:T'}$, Inputs $x_{1:T'}$, Prior: \mathbf{w}_0, σ_0 , Previous estimate of \mathbf{w} : \mathbf{w}^{old}
- 2: **Output:** $\{\mathbf{w}\}$
- 3: **function** GLMsampleposterior ($y_{1:T'}, x_{1:T'}, \mathbf{w}_0, \sigma_0, \mathbf{w}^{\text{old}}$)
- 4: $L(\mathbf{w}) = \sum_{t=1}^{T'} \log p(y = y_t \mid x_t, \mathbf{w})$
- 5: $\mathbf{w}^{\text{MAP}} \leftarrow \text{argmax}_{\mathbf{w}} (L(\mathbf{w}) + \log \mathcal{N}(\mathbf{w}; \mathbf{w}_0, \sigma_0^2 I))$
- 6: $C \leftarrow - \left(\frac{\partial^2 L(\mathbf{w})}{d\mathbf{w}^2} - \sigma_0^{-2} I \right)^{-1} \Big|_{\mathbf{w}^{\text{MAP}}}$
- 7: $\mathbf{w}^* \leftarrow \text{sample } \mathcal{N}(\mathbf{w}^{\text{MAP}}, C)$
- 8: $\alpha(\mathbf{w}^*, \mathbf{w}^{\text{old}}) \leftarrow \min \left(1, \frac{\tilde{p}(\mathbf{w}^* \mid y_{1:T'}, x_{1:T'}) \mathcal{N}(\mathbf{w}^{\text{old}}; \mathbf{w}^{\text{MAP}}, C)}{\tilde{p}(\mathbf{w}^{\text{old}} \mid y_{1:T'}, x_{1:T'}) \mathcal{N}(\mathbf{w}^*; \mathbf{w}^{\text{MAP}}, C)} \right)$ { \tilde{p} : unnormalized posterior}
- 9: **if** $\alpha(\mathbf{w}^*, \mathbf{w}^{\text{old}}) \geq U(0, 1)$ **then**
- 10: $\mathbf{w} \leftarrow \mathbf{w}^*$
- 11: **else**
- 12: $\mathbf{w} \leftarrow \mathbf{w}^{\text{old}}$
- 13: **end if**
- 14: **end function**

Algorithm 3 IO-HMM State sequence sampling

Input: Initial state dist. π , Transition matrix A , Likelihood matrix $L \in \mathbb{R}^{T \times K}$

Output: $z_{1:T}$

function IOHMMsamplestate (π, A, L)

$B \leftarrow$ HMM-Backwardmessages(A, L) $\{B_{t,k} = p(y_{t+1:T} \mid x_{1:T}, z_t = k)$ [7]}

$z_1 \leftarrow$ sample $\pi_k B_{1,k} L_{1,k}$ over $k \in \{1, \dots, K\}$

for $t \leftarrow 2, \dots, T$ **do**

$z_t \leftarrow$ sample $A_{z_{t-1},k} B_{t,k} L_{t,k}$ over $k \in \{1, \dots, K\}$

end for

end function

S8 Variational inference for IO-HMMs

For an IO-HMM with K distinct states and Bernoulli-GLM observations, we want to learn variational posteriors for the initial state distribution $\pi_0 \in \Delta^{K-1}$, the transition matrix $A \in \mathbb{R}^{K \times K}$ and the weights of the GLMs, $\mathbf{w}_{1:K} \in \mathbb{R}^D$. To do so, we use inputs to the model $\mathbf{x}_{1:T}$ and their corresponding observations $y_{1:T}$. The unknown latent states corresponding to these trials are represented by $z_{1:T}$.

Let's first first define prior distributions over the model parameters:

$$\pi_0 \sim Dir(\boldsymbol{\alpha}_0) \tag{S25}$$

$$A_{j,:} = \pi_j = \sim Dir(\boldsymbol{\alpha}_j) \quad j = 1 \dots K \tag{S26}$$

$$\mathbf{w}_k \sim \mathcal{N}(\mathbf{w}_0, \sigma_0^2 I) \quad k = 1 \dots K \tag{S27}$$

where $\boldsymbol{\alpha}_0 \in \mathbb{R}^K$ and $\boldsymbol{\alpha}_j \in \mathbb{R}^K$ and contain positive real numbers only, $\mathbf{w}_0 \in \mathbb{R}^D$, $\sigma_0 \in \mathbb{R}$. Now, let us define a variational posterior over the parameters and latent states of the IO-HMM as follows:

$$q(z_{1:T}, A, \pi_0, \phi_{k=1}^K) = q(z_1) \prod_{t=2}^T q(z_t \mid z_{t-1}) q(A) q(\pi_0) \prod_{k=1}^K q(\phi_k) \tag{S28}$$

Here, we assume that the latents are independent of the model parameters, which reflects the mean-field assumption. Next, we develop a coordinate ascent algorithm to iteratively learn the variational posteriors.

We will initialize $q(\pi_0)$, $q(A)$, $q(\mathbf{w}_k)$ to their prior distributions. Then, in the first step, we compute the following quantities:

$$\tilde{\pi}_0 = \exp\{\mathbb{E}_{q(\pi_0)}[\ln \pi_0]\} \tag{S29}$$

$$\tilde{A}_{j,:} = \exp\{\mathbb{E}_{q(A)}[\ln A_{j,:}]\} \tag{S30}$$

$$\tilde{L}_{t,k} = \exp\{\mathbb{E}_{q(\mathbf{w}_k)}[\ln p(y_t \mid \mathbf{w}_k, \mathbf{x}_t)]\} = \exp\left\{\frac{1}{N} \sum_{i=1}^N \ln p(y_t \mid \mathbf{w}_k^i, \mathbf{x}_t)\right\} \tag{S31}$$

The Dirichlet distributions over π_0 and $A_{j,:}$ provide closed form updates for $\tilde{\pi}_0$ and $\tilde{A}_{j,:}$ (in particular, for a D -dimensional vector $x \sim Dir(\boldsymbol{\gamma})$, $\mathbb{E}[\ln x_i] = \psi(\gamma_i) - \psi(\sum_i \gamma_i)$, where ψ is the digamma function). To compute $\tilde{L}_{t,k}$, which is not available in closed form in the case of GLM observations, we obtain a sample estimate of the expectations using 10 samples.

Next, using the quantities computed above, we run forward-backward algorithm for IO-HMMs [7], and obtain the forward and backward messages $F, B \in \mathbb{R}^{T \times K}$. This leads to the following

distributions over the latent states.

$$q(z_t = k) = F_{t,k} B_{t,k} / \left(\sum_{k'} B_{T,k'} \right) \quad (\text{S32})$$

$$q(z_{t-1} = j, z_t = k) = F_{t-1,j} \tilde{A}_{j,k} \tilde{L}_{t,k} B_{t,k} / \left(\sum_{k'} B_{T,k'} \right) \quad (\text{S33})$$

Now, we are ready to update the variational distributions over the model parameters:

$$q(\pi_0) \propto \prod_{k=1}^K \pi_{0k}^{\alpha_{0k} + q(z_1=k) - 1} \quad (\text{S34})$$

$$q(A) \propto \prod_{k=1}^K \pi_{jk}^{\alpha_{jk} + \sum_{t=2}^T q(z_{t-1}=j, z_t=k) - 1} \quad (\text{S35})$$

And finally, the variational approximation over the GLM weights is as follows:

$$q(\mathbf{w}_k) \propto \exp \left\{ \sum_{t=1}^T q(z_t = k) \ln p(y_t | \mathbf{w}_k, \mathbf{x}_t) + \ln p(\mathbf{w}_k) \right\} \quad (\text{S36})$$

Unlike typical Gaussian HMMs, this is not available in closed form because the likelihood of a Bernoulli-GLM does not have a conjugate prior. To deal with this, we approximate $q(\mathbf{w}_k)$ by a Gaussian distribution using Laplace approximation. Let $L(\mathbf{w}_k) = \exp \left\{ \sum_{t=1}^T q(z_t = k) \ln p(y_t | \mathbf{w}_k, \mathbf{x}_t) + \ln p(\mathbf{w}_k) \right\}$.

$$q(\mathbf{w}_k) \sim \mathcal{N}(\mathbf{w}'_k, \Sigma'_k); \quad \mathbf{w}'_k = \operatorname{argmax}_{\mathbf{w}_k} L(\mathbf{w}_k), \quad \Sigma'_k = \left(\frac{\partial^2 L(\mathbf{w}_k)}{\partial \mathbf{w}_k^2} \right)^{-1} \Big|_{\mathbf{w}'_k} \quad (\text{S37})$$

We repeat the update equations from eq. S29 to eq. S37 iteratively until the log-likelihood of the data from the model converges or a maximum of 500 iterations is reached.

Once we have obtained a variational distribution for all the model parameters, we can draw M samples of $\{\pi_0^j, A, \mathbf{w}_{1:K}^j\}_{j=1}^M$ from their variational posteriors. We set $M = 500$ for our experiments.

S9 Additional analyses for IO-HMMs

Here, we compare our infomax learning method using variants of Gibbs sampling. In all our experiments in sec. 5, we run a single chain to obtain 500 samples of the model’s parameters, discarding the initial 200 burn-in samples. If we instead run 5 parallel chains, each of length 140 and discard the first 40 samples as burn-in, we would still be able to obtain 500 samples of the model parameters to perform infomax learning, but this provides a 5X improvement in speed, leading to ~ 4 secs per trial for input selection. We verify in Fig. S2 that the perform of infomax while using parallel chains of Gibbs is comparable to that using a single long chain (compare the red and violet traces).

Finally, in all our experiments, we use our Laplace-based Gibbs sampling approach for IO-HMMs (detailed in sec. S7). We compared this to Polya-Gamma augmented Gibbs sampling [51, 54], an

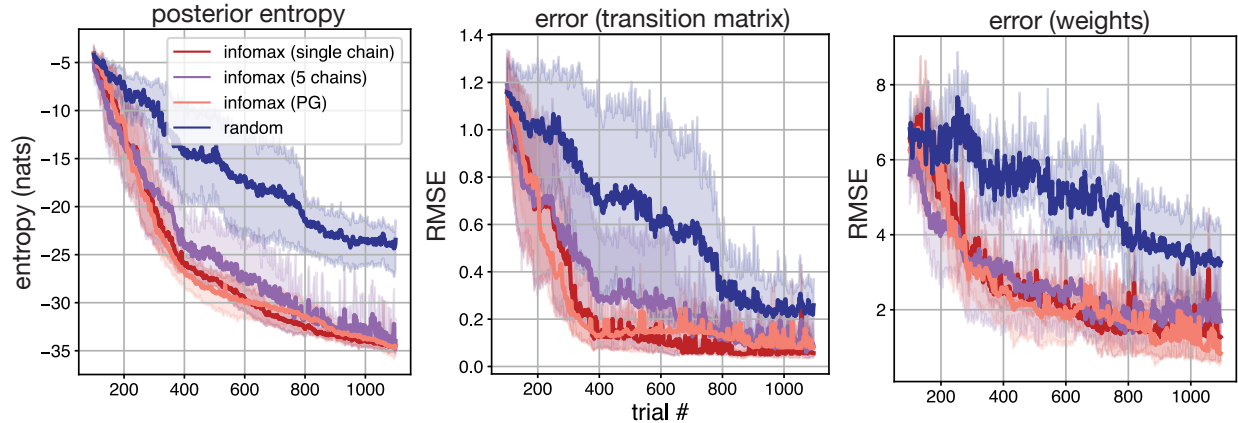


Figure S2: Infomax learning for IO-HMMs. Left panel shows the posterior entropy of model parameters over the course of 1000 trials when performing infomax learning using our Laplace-based Gibbs sampling approach with a single long chain (red), using parallel chains of our Laplace-based Gibbs sampler (violet), using Polya-Gamma augmented Gibbs sampling (peach), and using random sampling (blue). Middle and right panels show error in recovering the transition matrix and the weights of the GLMs using the same set of methods.

established technique in the literature to sample from logistic models. In this case, weights of the GLM are sampled using Polya-Gamma augmentation, while the strategy for sampling the latents and the state transitions remain the same as in algorithm 1. We show in Fig. S2 that our approach is comparable to Polya-Gamma augmentation in terms of both posterior entropy and error in recovering the model parameters (compare the peach and red curves). This empirically verifies the utility of our Laplace-based Gibbs sampling approach for IO-HMMs.

S10 Infomax for Mixture of GLMs (MGLMs)

We evaluate infomax on a special case of IO-HMMs: a mixture of Bernoulli-GLMs (MGLMs). Compared to standard IO-HMMs, MGLMs assume that the probability that the system transitions to state k at trial $t + 1$ is independent of the system’s state at trial t . MGLMs arise in a number of settings including in medicine, transport modeling and in marketing [20–22, 42, 62]. Formally, MGLMs contain K distinct GLM observation models where the state of the model, $z \in \{1, \dots, K\}$, is independently sampled at each time step from a distribution $\pi \in \Delta^{K-1}$. Similar to the IO-HMM setup, observations are generated according to a Bernoulli GLM as in Eq. 6. Infomax learning using Gibbs sampling for MGLMs involves similar steps to those required for IO-HMMs and is described in S11.

We perform an experiment to assess the effectiveness of our active learning method in this setting. Data was generated from a 2-state MGLM model (shown in Fig. S3A) with $\pi = [0.6, 0.4]$ and the GLM weights $w_1 = [3, -6], w_2 = [3, 6]$. We find that our active learning method is better than random sampling at inferring the parameters of this model (Fig. S3B, C).

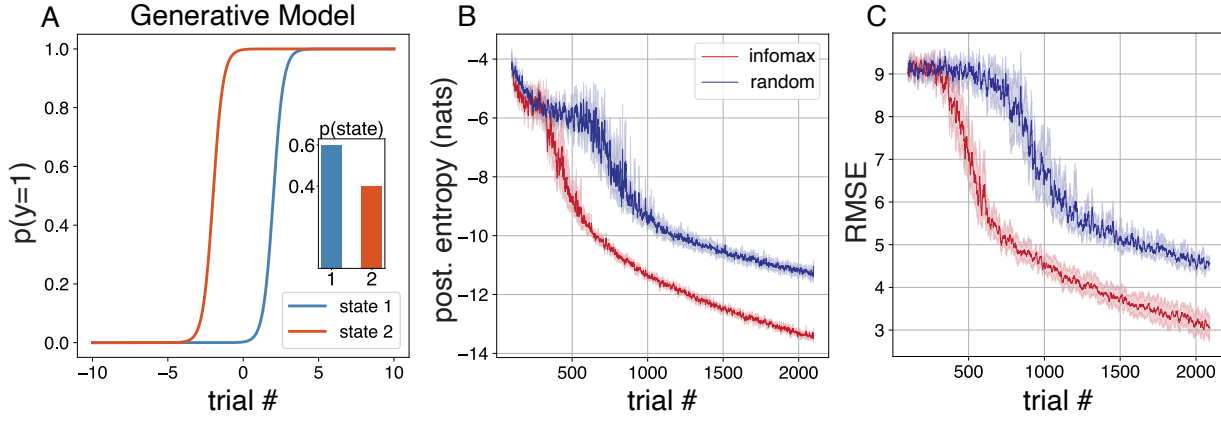


Figure S3: Infomax learning for mixture of GLMs (MGLMs): (A) Data generation model. Example settings for a 2-state MGLM along with the mixing weights for the two states. (B) Posterior entropy of model parameters over the course of 2000 trials for random sampling (blue) and infomax learning for MGLM (blue). (C) Root mean squared error for the recovered GLM weights and mixing weights for each of the two input-selection schemes.

S11 Gibbs Sampling for MGLMS

Gibbs sampling for MGLMs is similar to that for IO-HMMs except that now the states can be sampled independently of each other. Algorithm 4 provides full details. We set a Dirichlet prior over the initial state distribution, with $\alpha_0 = \mathbf{1} \in \mathbb{R}^K$, and that over the weights to be $\mathcal{N}(\mathbf{0}, 10)$. Here, we run Gibbs sampling for 700 iterations and discard the first 200 as burn-in (MGLMs require a longer burn-in period).

Algorithm 4 MGLMs Gibbs Sampling

- 1: **Input:** Observations $y_{1:T}$, Inputs $\mathbf{x}_{1:T}$, Priors: $\alpha_0, \mathbf{w}_0, \sigma_0$
 - 2: **Output:** Samples $\{(z_{1:T}, \mathbf{w}_{1:K}, \pi)^{(j)}\}$
 - 3: Initialize $z_{1:T}, \mathbf{w}_{1:K}, A, \pi$
 - 4: **for** $j \leftarrow 1, \dots, M$ **do**
 - 5: **for** $k \leftarrow 1, \dots, K$ **do**
 - 6: $\mathbf{w}_k^j \leftarrow \text{GLMsampleposterior}(\{y_t, \mathbf{x}_t \mid z_t = k\}_{1:T}, \mathbf{w}_0, \sigma_0, \mathbf{w}_k^{j-1})$
 - 7: **end for**
 - 8: $\pi^j \leftarrow \text{sample Dir}(\alpha_0 + \mathbf{n})$ {where $n_k = \sum_t \mathbf{I}(z_t = k)$ }
 - 9: $z_t^j \leftarrow \text{sample } p(z_t \mid y_t, \mathbf{x}_t) \forall t = \{1 : T\}$ {s.t. $p(z_t = k \mid y_t, \mathbf{x}_t) = \frac{p(y=y_t \mid \mathbf{x}_t, \mathbf{w}_k) \pi_k}{\sum_k p(y=y_t \mid \mathbf{x}_t, \mathbf{w}_k) \pi_k}$ }
 - 10: **end for**
-